Output from Linear Generator for VIV-driven Buoy

Wayne Liu, Jack Dea, Kyle Wendler, Brian Dick,
SPAWAR Systems Center Pacific (SSC Pac)
San Diego, CA (USA)
Wayne.P.Liu@navy.mil

Brian D’Angelo
American Society of Engineering Education (ASEE)
Washington, D.C. (USA)

***Abstract*—We present test data of a linear generator design that could be integrated within a submerged tethered buoy. Machine and hand driven magnet actuation demonstrated power outputs which could be achieved with a pendulum drive mechanism within a buoy undergoing Vortex Induced Vibrations. We also model the range of VIV excitation and natural frequencies that can be achieved for a tethered buoy with an internal pendulum mechanism.**

***Index Terms*—Vortex Induced Vibrations, buoy, linear generator, pendulum, modeling**

I. Introduction

Within the offshore structural and civil engineering communities, Vortex Induced Vibrations (VIV) are often responsible for annoying acoustical tones or in extreme cases, outright structural failures. Thus, much work has been focused over the past few decades in designing structures to minimize or defeat VIV. However, one area in which VIV is most welcome is in the field of energy harvesting. In this application, VIV can be exploited and even amplified to oscillate magnetic fields against coils to generate voltage and thus power.

Large scale demonstration of VIV based energy harvesting was accomplished by Bernitsas of Vortex Hydro Energy and their Vortex Induced Vibration Aquatic Clean Energy (VIVACE) platform, which was installed in the St. Clair River in Port Huron, MI [1]. This particular platform used river flow to drive an array of large diameter, vertically oscillating cylinders and sought to prove the viability of tapping low speed water flows for commercial power. Small scale commercial demonstration of vortex or flow induced vibrations in air was performed by Frayne [2] using the Wind Belt, which would oscillate end-mounted magnets in and out of coils.

While previous designs have shown that significant power can be harvested from VIV, there are still many design considerations which have yet to be answered. For instance, how could VIV be exploited for generating power in deeply submerged ocean applications where slow current flow (0.5 kts), changing flow directions and ease of deployment and maintenance are critical drivers of any design? To address this problem, SPAWAR Systems Center Pacific (SSC Pac) has conducted research using small (0.5” diam) and large scale (10” diam) cylinders to produce VIV for power generation.

FY13 work (see Fig. 1) evaluated the feasibility of 1W power output from a linear magnetic generator that can fit inside a 10 - 12” (0.25 – 0.30 m) diam buoy and be driven by VIV in 0.5 kts (0.25 m/s) flow. Additional work at SSC Pac will design a pendulum drive within a buoy to actuate the linear generator.

This paper will discuss: 1) power output that can be expected when cycling a pair of 2” spherical neodymium magnets within a PVC pipe fitted with multiple coil structures and 2) predictions of buoy oscillation frequencies that can be used to actuate an internal pendulum device for driving magnet/coil structures.

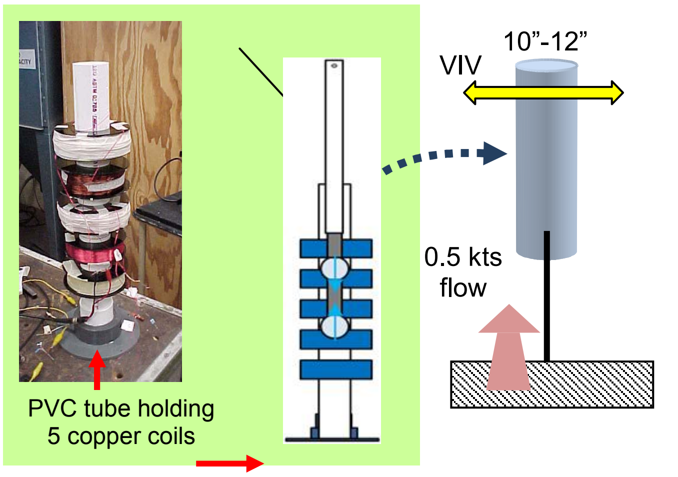

***Fig. 1.** FY13 work seeks to evaluate feasibility of 1W power output from linear generator that can fit inside a 10” - 12” diam buoy and be driven by Vortex Induced Vibrations (VIV) in 0.5 kts flow.*

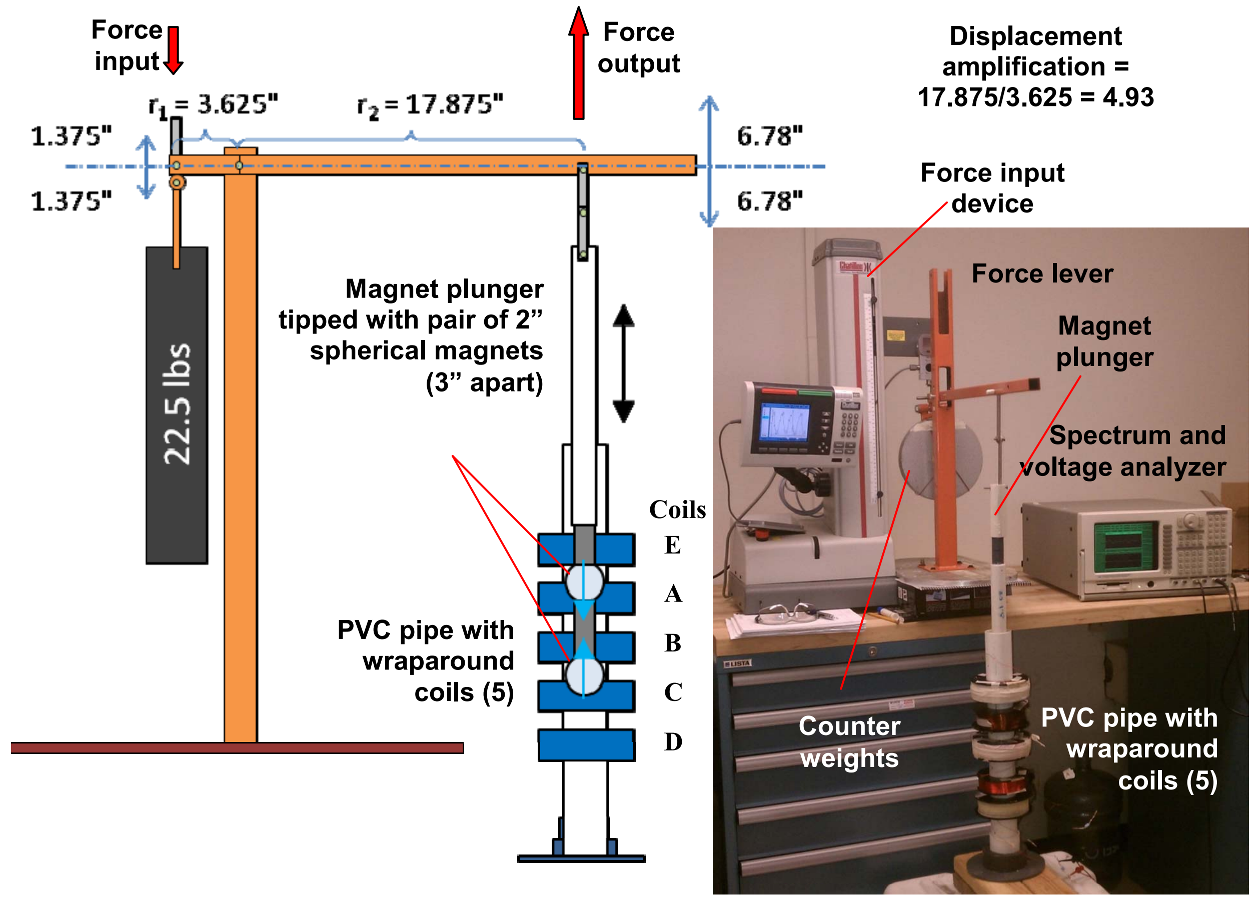

Fig. 2. *Test setup for evaluating linear generator consisting of spherical magnet pair driven in/out of PVC pipe fitted with wraparound coils. Input force was controlled and measured by benchtop actuation device; voltage output of coils (open circuit and loaded) recorded by spectrum analyzer device.*

II. LINEAR GENERATOR

To characterize a linear generator arrangement that could likely be integrated within and driven by VIV oscillations of an upright tethered buoy, a test setup was constructed to measure magnet travel, actuation force and resultant voltage outputs across a series of copper coils. Figure 2 shows a photo and the dimensions of the setup, including force input and measurement device (Chatillon TCD225 Force Measurement system), lever arm for amplifying displacement input, magnet plunger, and PVC pipe with copper coils

Since the total actuation distance of the force input device was limited to 2.75", a lever arm was used to amplify the stroke input by 4.93X to raise the magnet plunger ±6.78" above and below the horizontal axis (total 13.56" stroke distance). The magnet plunger served to drive two 2" diameter neodymium magnet spheres (separated by a 3" spacer) in/out of a 2.0" ID PVC pipe, upon which five copper coils were affixed.

Figure 3 shows force input over time/distance for driving the pair of magnet spheres up and down:

a) without any constraining PVC pipe structure
b) inside the PVC pipe and with the coils unloaded
c) inside the PVC pipe with resistor loads across the coils.

Table 1 lists the characteristics of the five coils wrapped around the PVC pipe.

Table 1. *Diameter, resistance and turns of wraparound coils on PVC pipe*

Coil	Diam (in)	Resistance (ohms)	Turns
E	5	33	1560
A	4.5	55	1560
B	5	33	1560
C	4.25	220	2600
D	4.5	55	1560

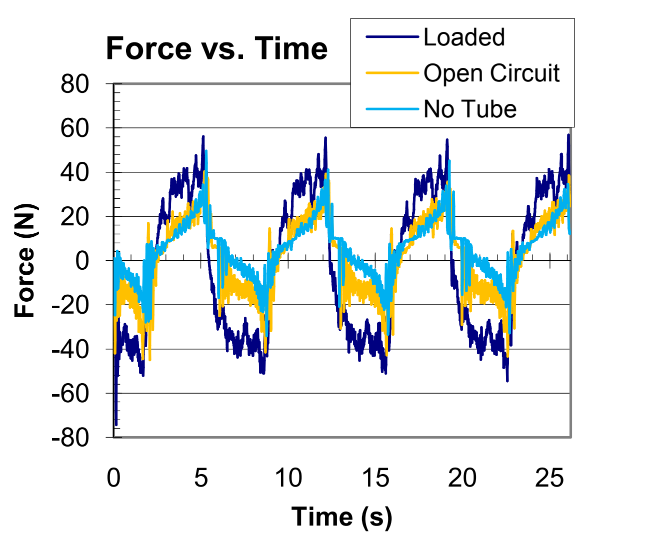

Fig. 3. *Force applied at short end of lever arm over several cycles to actuate magnet plunger with various loading conditions. Actual force in driving magnet plunger is 4.9X less due to lever arm used to amplify displacement (see Fig. 2).*

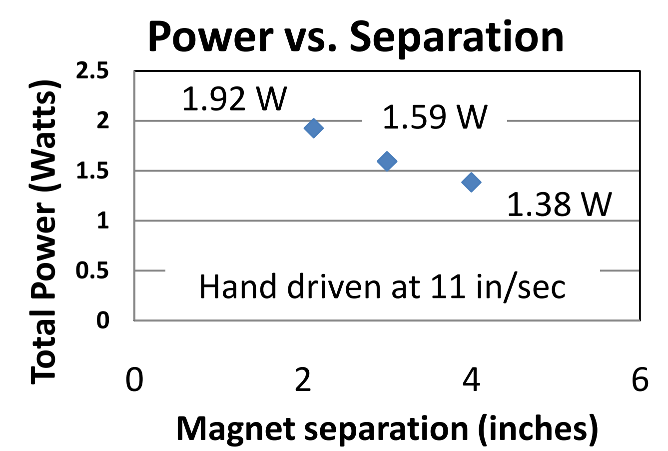

Fig. 4. *Testing of linear generator showed that roughly 1 – 2W is possible when a pair of magnet spheres (2" diam) is hand driven up/down through a five coil array at a rate of ~11 in/sec. Power is increased when magnet pair is brought closer together from 4" to 2.125", creating a more compressed flux gradient and thus greater power generation when passing a coil.*

With matched resistor loads attached to the coils, a maximum force of 50-55 N was delivered by the machine at the short end of the lever arm to actuate the magnet plunger; this translated to a maximum lifting force of 10-11 N (4.9X less) imposed directly over the magnet plunger. The resultant power output (RMS) was measured to be 0.148W by summing the outputs (V^2/R) of the five resistors during a complete displacement cycle for the magnet plunger. A plunger displacement cycle consisted of two 13.6" strokes (down/up) covered in 6.6 sec (~4"/sec).

To evaluate power output when actuating the magnet plunger at a faster rate than the machine's maximum output of 27.2" (13.6"/stroke x 2 strokes) per 6.6 sec, the plunger was disconnected from the lever arm and manually driven down and back up within the PVC pipe in 2.5 sec (~11"/sec). Granted, this hand-driven magnet actuation is not precise, but serves only to provide a rough measure of what power is available when magnet actuation speed is increased.

Figure 4 shows the resultant power output when the pair of magnet spheres was hand driven while separated by 4.0", 3.0", and 2.125" steel spacers. Figure 4 shows that 1.38 – 1.92 W was achieved when plunging a single pair of 2" diam spherical magnets past a five coil array at speeds of roughly 11" per second.

When magnet pair separation is reduced from 4" to 2.125", greater power is captured across the five coils (from 1.38 to 1.92W). This is likely due to the compression of the flux gradient between the two magnets, resulting in greater power. Flux compression is used in SSC Pac developed Kinetic Energy Harvesters (KEH's) to increase power output [3].

III. MODELING VIV OSCILLATIONS

The linear generator testing demonstrated what range of power output is achievable for a buoy compatible magnet/coil structure and magnet actuation force and speed inputs. Using this force and speed data as a design goal, we can begin to model a submerged tethered buoy to yield VIV oscillations for driving an internal pendulum actuator.

A. Modeling Buoy Excitation and Natural Frequencies

Oscillation of a tethered submerged buoy can be optimized by synchronizing or matching its vortex shedding or flow excitation frequency (f_{vs}) to its natural or resonant frequency (f_b). However, the presence of a significant pendulum load inside the buoy will couple into the overall buoy oscillation and shift buoy resonant frequency (f_{bp}) according to buoy mass (m_b), pendulum spring constant (k) and pendulum mass (m_p). Figure 5 illustrates the myriad of variables at play which will produce the various oscillation frequencies that must be aligned to optimize buoy motion.

The frequency of flow excitation (vortex shedding, f_{vs}) on submerged bodies can be determined by the well known Strouhal number (St), which relates f_{vs}, the cylinder diameter (D), and cross flow velocity (U) to a Reynolds number (Re) dependent coefficient [4,5]. For a cylinder in a wide range of flow conditions leading to a Reynolds number (Re) of 300 to 10^5, equation (1) shows that St can be approximated as 0.20 (Ball et. Al. 2012).

$$St = \frac{f_{vs} D}{U} = 0.20 \quad (1)$$

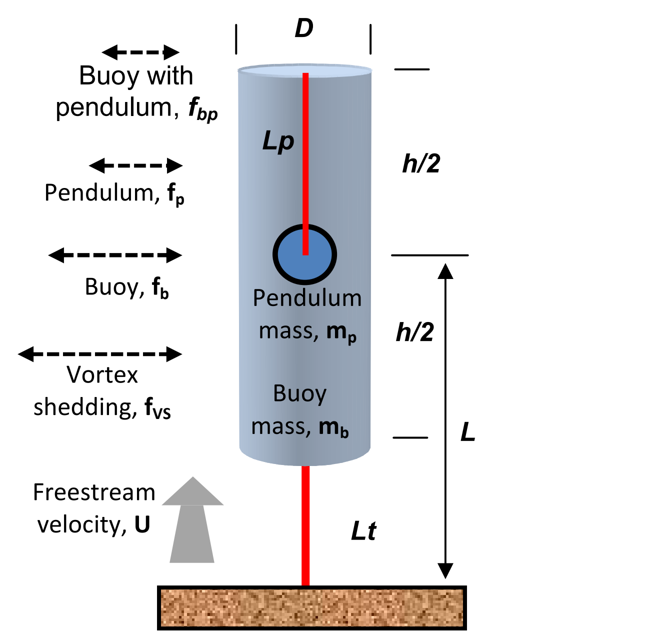

***Fig. 5.** To optimize buoy oscillations for actuating an internal pendulum drive, various structural frequencies must be matched against vortex shedding frequencies by adjusting buoy and pendulum mass. Modeling methods will be presented that can be used to align such frequencies.*

For flows in the scope of this research, where nominal D = 0.25 m and water velocity U = 0.25 m/s, Re = 62,500 and the flow excitation frequency f_{vs} is estimated by Strouhal number to be 0.20 Hz or one oscillation cycle per five sec. To optimize buoy oscillations for power generation, buoy and pendulum natural frequencies should be designed to match f_{vs}.

The natural frequency of a pendulum can be easily determined by equation (2). This equation shows the angular frequency ω as a function of the spring constant k and the total mass M. The spring constant of a tethered buoy is given by equation (3). In this equation, m_b is the mass of the buoy, g is the gravity constant, and L is the length of the buoy tether when extended to the center of gravity. It is important to differentiate between total mass and buoy mass. Since this buoy will be completely submerged, it is important to account for the added mass of the buoy (m_a). Therefore, the total mass M is a combination of the added mass (m_a) and the buoy mass (m_b) shown in equation (4) [6].

$$(2) \qquad \omega = \sqrt{\frac{k}{M}}$$

$$(3) \qquad k = \frac{m_b g}{L} \qquad \text{(hanging pendulum)}$$

$$(4) \qquad M = m_b + m_a$$

The added mass m_a is easily calculated by the equation below provided by Berteaux [7]. Note that every shape has an individual equation for added mass and equation 5 describes the added mass of a cylinder.

$$(5) \qquad m_a = \rho_w V C_a$$

In equation (5) above, ρ_w is the fluid density, V is the volume of the cylinder, and C_a is the added mass coefficient (typically 1 for a cylinder).

In equation (3) above, it is important to note that this is the spring constant of a hanging pendulum. The buoy, however, will essentially be an inverted pendulum. Comparison of the free body diagrams in figure 6 show how the spring constant should be adjusted to account for an inverted pendulum with a positively buoyant mass.

Using the methodology presented by Colwell (see Fig. 6), the spring constant for a submerged, inverted pendulum is shown below in equation (6). Simply put, this equation states that the spring constant of an inverted pendulum is the difference between the buoyant and gravitational forces divided by the pendulum length (measured to center of mass).

$$(6) \qquad k = \frac{(\rho_w V - m_b)g}{L}$$

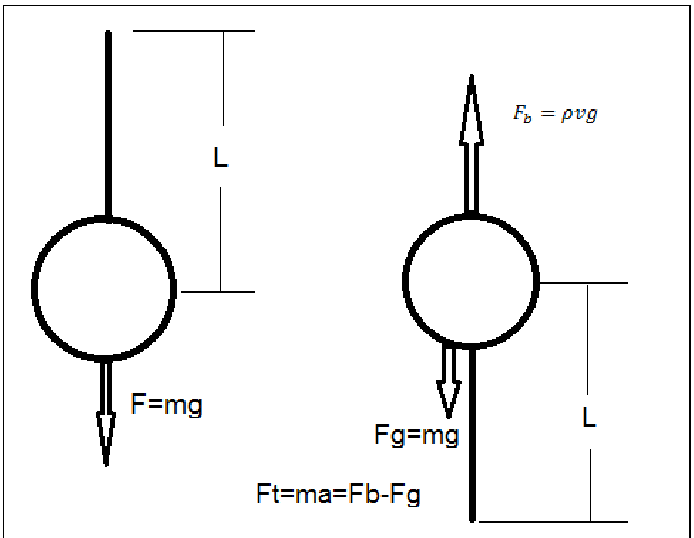

***Fig. 6.** Free body diagrams of (left) heavy or negatively buoyant pendulum and (right) light or positively buoyant pendulum.*

Plugging equations 4, 5, and 6 into equation 2 will provide the natural frequency of a submerged buoy assuming no damping and no internal spring. This is shown in equation (7) below.

$$(7) \qquad \omega_b = \sqrt{\frac{(\rho_w V - m_b)g}{(m_b + \rho_w V C_a)L}}$$

Recognizing that m_b will always be a fraction of $\rho_w V$ for a positively buoyant object, we can make use of a mass ratio m* that is often used by VIV researchers [8,9] to relate the mass of oscillating parts to the mass of the fluid displaced by the oscillating parts. A mass ratio less than 1 indicates a positively buoyant VIV platform, whereas m* = 3 indicates the oscillating parts are 3X heavier than their displaced fluids.

Essentially, $m^* = m_b/m_{fd}$. Then replacing m_b with $\rho_w V m^*$, equation (7) can be reduced to:

$$\omega_b = \sqrt{\frac{(1-m^*)g}{(m^*+C_a)L}} \tag{8}$$

Equation (8) shows that buoy natural frequency ω_b is a function of m* (ratio of buoy mass to displaced fluid mass), the gravity constant, and length of tether to the center of buoy mass and is independent of buoy diameter D.

B. Buoy with Internal Pendulum Load

While equation (8) describes the natural frequency of a submerged buoy, the design presented in this paper seeks to utilize an internal pendulum to drive a linear generator and thus introduces a secondary, internal spring-mass system. The entire system can be graphically represented by a system of springs and masses connected in series (see Fig. 7).

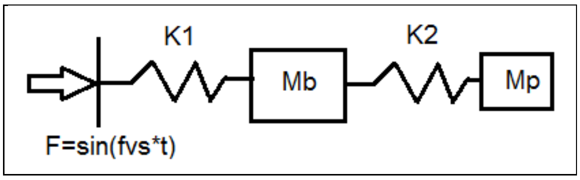

Fig. 7. *Spring-mass diagram for buoy mass, Mb and internal pendulum mass, Mp undergoing VIV driven excitation.*

This graphical representation shows a forcing frequency acting on two spring mass systems in series. As conventional physics describes, there will be a coupling effect due to the second spring-mass system acting on the first spring-mass system and vise versa. Note that for the time being, all damping forces have been neglected. Deriving the effect of this coupling on the natural frequency of the system has been done by Electro-Standards Laboratory and the University of Rhode Island in 2008 by deriving a 'resonance match condition'. Using the equation presented in their STTR report[10], and plugging in equations 4, 5, 6 and 7, equation (9) was derived.

$$\omega_{match} = \frac{\sqrt{(\omega_b+\omega_p)^2+\frac{gm_p}{L_2M}} - \sqrt{(\omega_b-\omega_p)^2+\frac{gm_p}{L_2M}}}{2} \tag{9}$$

Equation (9) solves for the angular frequency of the resulting system due to a coupled spring-mass system. In this equation, the second term within each radical, $\frac{gm_p}{L_2M}$, represents the inertial effect of the internal spring constant on the total mass of the buoy. In this term, g is gravity, m_p is the mass of the internal pendulum, M is the total mass of the buoy ($m_b + \rho_w V m^* C_a$) and L_2 is the length of the internal pendulum. ω_b is the angular natural frequency of the buoy given by equation 8. ω_p is the angular frequency of the internal pendulum given by equation (10) below.

$$\omega_p = \sqrt{\frac{g}{L_2}} \tag{10}$$

Recognizing that m_p will always be a fraction of m_b when an internal pendulum load is carried within the buoy, we can utilize a ratio p^* defined as the mass of the internal pendulum load m_p relative to the mass of the buoy, m_b. Thus for a fixed or non-moving pendulum load within a buoy, p* = 0, whereas p* = 0.8 indicates that the free swinging pendulum mass constitutes 80 percent of the buoy mass.

Essentially, $p^* = m_p/m_b$. Then replacing m_p with $m_b p^*$ and m_b with $\rho_w V m^*$, Equation (9) can be reduced to

$$\omega_{match} = \frac{\sqrt{(\omega_b+\omega_p)^2+\frac{gp^*m^*}{L_2(m^*+C_a)}} - \sqrt{(\omega_b-\omega_p)^2+\frac{gp^*m^*}{L_2(m^*+C_a)}}}{2} \tag{11}$$

Equation (11) defines the resultant natural frequency of a buoyant tethered buoy with a free-swinging internal pendulum load in terms of p*, m*, Ca (typically 1 for cylinder), ω_b and ω_p. Similar to Equation (8), this natural frequency is not affected by buoy diameter D, but is driven by the buoy and pendulum mass relative to displaced fluid mass (m* and p* respectively) and length of the internal pendulum, L2.

Figure 8 plots this ω_{match} as a function of m* and family of curves representing a range of p* values. For a 0.25 m diam x 0.60 m long buoy in 0.25 m/s flow, a vortex shedding frequency, f_{vs} of 0.20 cycles/sec is calculated using the Strouhal number relationship in Equation (1). To have any chance of matching this excitation frequency, buoy and pendulum masses must be adjusted against displaced fluid mass. For example:

m* = 0.65 for a fixed pendulum load (p* = 0), or
m* = 0.40 for a pendulum mass ratio p* of 0.1

This model currently excludes any effects of damping. As conventional physics describes, the natural frequency of a pendulum will be shifted by a damping effect. This shift is described by equation 12 below. In this equation, ω_{peak} is the new, shifted natural frequency of the system, ω_{match} is the non-damped natural frequency of the buoy with an internal pendulum mass, and ζ is the damping coefficient. For the internal pendulum, this will be an appropriate assumption until the electrical and mechanical damping from the generator is introduced to the system. For the buoy natural frequency, this assumption should hold true as the predicted velocities of the buoy's oscillation are fairly small. The damping coefficient will be determined experimentally later at SSC Pac.

$$\omega_{peak} = \sqrt{1-\zeta^2}\,\omega_{match} \tag{12}$$

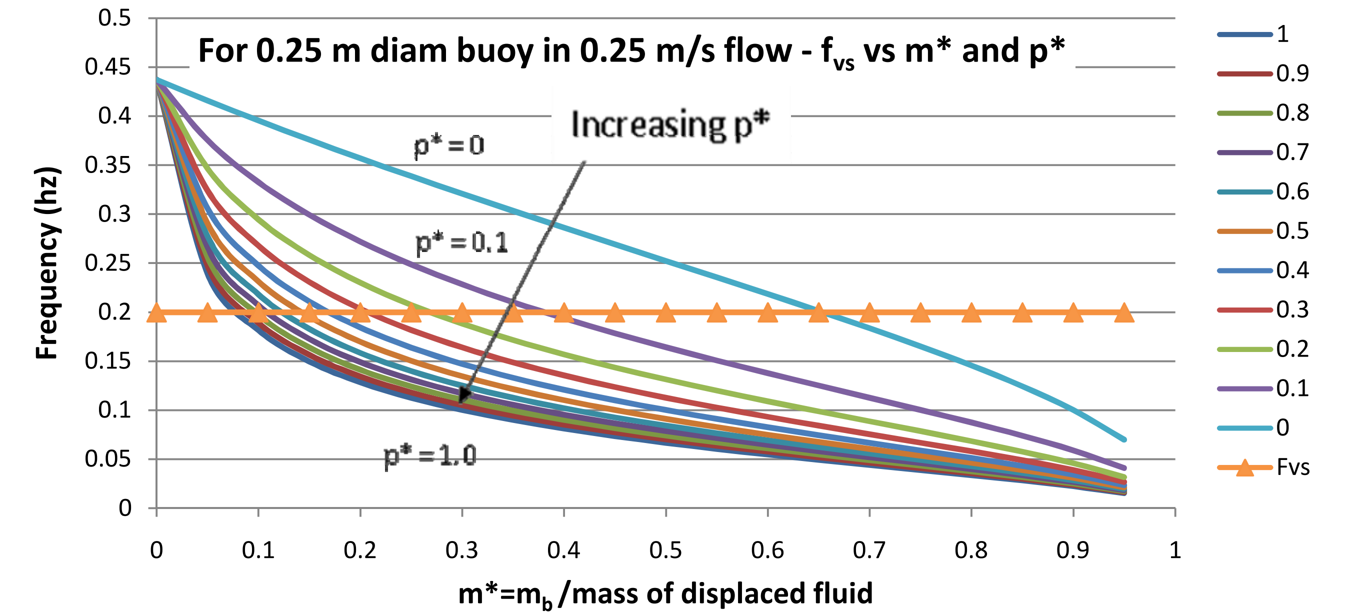

Fig. 8. *Natural frequency for range of m* (m_b/mass of displaced fluid) and p* (pendulum mass/buoy mass) ratios are modeled. Excitation frequency f_{vs} is fixed (horizontal line) for given buoy diameter and flow velocity; f_{vs} matches natural buoy frequencies at line intersections.*

IV. CONCLUSIONS

A derivation of a non-dimensionalized math model was presented for predicting oscillation frequencies of a submerged tethered buoy. The model included a prediction of the buoy excitation frequencies due to vortex shedding. To match this excitation frequency with buoy natural frequencies, this model included coupling effects of an internal pendulum and added mass of the buoy, but excluded viscous damping. This model did not include coupling of the buoy motion on the vortex shedding frequencies.

This paper also presented a linear generator system which could be used internally in an upright buoy to produce power. Simple power tests were conducted using machine and manual actuation of the magnets.

Future work on this project will include: a), laboratory and field testing to validate the VIV oscillation model, b) if needed, the model will be adjusted to include a coupling effect of buoy motion with vortex shedding as well as viscous damping, and c) a generator will be incorporated into a buoy design to validate power output predictions. The effects of the generator on the model will the then be included.

ACKNOWLEDGEMENTS

The authors are grateful for the SSC Pac Internal R&D support provided by Dr. Dave Rees and the Office of Naval Research In-Laboratory Independent Research (ILIR) program. This research would not have been possible without the superb support and insight provided by Charles Coughran, Dave Aglietti, and John Lyons of the Scripps Institute of Oceanography Hydraulics Lab (La Jolla, CA).

REFERENCES

[1] VIVACE, www.vortexhydroenergy.com/developments/, accessed 30 July 2013.

[2] Wind Belt, www.popularmechanics.com/science/energy/solar-wind/4224763 accessed 30 July 2013.

[3] A. Phipps, D. Phung, M. Kerber, B. Dick, A. Powers, R. Waters, "Development of Kinetic Energy Harvesting Systems for Vehicle Applications", http://ieeexplore.ieee.org/stamp/stamp.jsp?arnumber=06127010

[4] M. R. Gharib, "Vortex Induced Vibration, Absence of Lock-in, and Fluid Force Deduction." Thesis. California Institute of Technology, 1999. Web 6 June 2013.

[5] R. D. Blevins, *Flow-induced Vibration*. 2nd ed. New York: Van Nostrand Reinhold, 1990. Print.

[6] C. H. Colwell, "PhysicsLAB." *PhysicsLAB*. N.p., n.d. Web. 10 June 2013.

[7] H. O. Berteaux, *Coastal and Oceanic Buoy Engineering*. Woods Hole, MA (P.O. Box 182, Woods Hole 02543): H.O. Berteaux, 1991.

[8] A. Khalak, C.H.K. Williamson, "Motions, Forces, and Mode Transitions in Vortex-Induced Vibrations at low mass-damping", *Journal of Fluids and Structures* (1999) 13, 813-851

[9] R. D. Blevins, C. S. Coughran, "Experimental Investigation of Vortex-Induced Vibration in One and Two Dimensions With Variable Mass, Damping, and Reynolds Number", *J. Fluids Eng.* 131(10), 101202 (Sep 30, 2009)

[10] Electro Standards Laboratories, "Ocean Energy Extraction for Sensor Applications", STTR Phase I Final Technical Report, Contract N00014-08-M-0277, 20 Feb 2009